Frascati Physics Series Vol. LVI (2012)
Dark Forces at Accelerators
October 16-19, 2012

U BOSON SEARCH IN THE $e^+ + e^- \to \mu^+\mu^-\gamma$ PROCESS AT KLOE

F. Curciarello
Dipartimento di Fisica e di Scienze della Terra, 98166 Messina, Italy
INFN-Sezione Catania, I-95123, Catania, Italy
On behalf of KLOE/KLOE2 Collaboration *

Abstract

Following recent puzzling astrophysical results and recent theoretical studies, a search for a relatively low mass (1 GeV) new vector gauge boson (called the U boson), weakly coupled with SM particles and decaying into lepton pairs, by using the Initial State Radiation (ISR) process, was performed at KLOE. 239.29 pb^{-1} of data were used to search for light vector boson in the $e^+e^- \to \mu^+\mu^-\gamma$ channel. No evidence was found and a preliminary upper limit in the $600 - 1000\,MeV$ mass range was extracted.

* D. Babusci, D. Badoni, I. Balwierz-Pytko, G. Bencivenni, C. Bini, C. Bloise, F. Bossi, P. Branchini, A. Budano, L. Caldeira Balkeståhl, G. Capon, F. Ceradini, P. Ciambrone, F. Curciarello, E. Czerwiński, E. Dané, V. De Leo, E. De Lucia, G. De Robertis, A. De Santis, P. De Simone, A. Di Domenico, C. Di Donato, R. Di Salvo, D. Domenici, O. Erriquez, G. Fanizzi, A. Fantini, G. Felici, S. Fiore, P. Franzini, P. Gauzzi, G. Giardina, S. Giovannella, F. Gonnella, E. Graziani, F. Happacher, L. Heijkenskjöld, B. Höistad, L. Iafolla, E. Iarocci, M. Jacewicz, T. Johansson, K. Kacprzak, W. Kluge, A. Kupsc, J. Lee-Franzini, F. Loddo, P. Lukin, G. Mandaglio, M. Martemianov, M. Martini, M. Mascolo, R. Messi, S. Miscetti, G. Morello, D. Moricciani, P. Moskal, S. Muller, F. Nguyen, A. Passeri, V. Patera, I. Prado Longhi, A. Ranieri, C. F. Redmer, P. Santangelo, I. Sarra, M. Schioppa, B. Sciascia, M. Silarski, C. Taccini, L. Tortora, G. Venanzoni, R. Versaci, W. Wiślicki, M. Wolke, J. Zdebik

1 Introduction

In the last decades one of the main goal of particle physicists and astrophysicists was to shed light on the possible existence of dark matter and dark energy. Usually, experiments are mainly oriented towards the discovery of new particles at high energy scales, however, a complementary interesting approach is the search for new light particles at relatively low energy scales. Such particles may have remained undiscovered because of their weak coupling to the Standard Model (SM). Moreover, in the last two years striking astrophysical observations, that cannot be interpreted by standard Astrophysics and Particle Physics, have attracted particular attention of the Scientific Community on the study of a hidden low–energy dark sector. Among the most important we remind observations by PAMELA [1)], INTEGRAL satellite [2)], ATIC [3)], Hess [4)], Fermi [5)] and DAMA/LIBRA [6)]. The most interesting thing is that all these observations could be explained if one assumes that a dark force gauge boson, mediator of an unknown force with mass less than two proton mass, $M_U < 2\,m_p$, exists. The U boson, also called dark photon, is predicted by several Standard Model Extensions (SME) [7, 8, 9, 10, 11, 12)]. According to dark force models this dark force gauge boson would be produced during dark matter annihilation processes and then decay into light particles, as leptons, ($\tilde{X} + X \to U + U$, $U \to l^+ l^-$, $l = e, \mu$), assuming a mass less than 1 GeV [13)]. Such dark photon is associated to an abelian gauge symmetry that can communicate with the ordinary SM through a kinetic mixing term that is given by the following relation: [7, 8, 13, 14)]

$$L_{mix} = -\frac{\varepsilon^2}{2}\, F_{ij}^{e.m.}\, F_{dark}^{ij} \tag{1}$$

where $\varepsilon^2 = \alpha^{'}/\alpha$ is the kinetic mixing parameter ($\alpha = 1/137$, $\alpha^{'}$ is the U boson coupling constant), $F_{ij}^{e.m.}$ is the electromagnetic tensor, F_{dark}^{ij} is the dark matter hypercharge gauge boson tensor.

Luckily, dark force models make a number of predictions that can be tested by particle physics experiments. Particularly, high luminosity $e^+ - e^-$ collider experiments at GeV scale can be a direct probe of dark forces. At flavour factories a particular clean channel is the production of the U boson plus a photon with the consequent decay of the U boson in a lepton pair:

$e^+e^- \to U\gamma \to l^+l^-\gamma$, where $l = e, \mu$ [13]. The expected U boson signal should have the shape of a Breit-Wigner peak in the invariant mass distribution of the lepton pair. For this reason, about $240\,pb^{-1}$ of KLOE data taken on 2002 were used to analyse the $e^+e^- \to \mu^+\mu^-\gamma$ channel with the aim to search for the light vector gauge boson.

2 KLOE Experimental Set Up

DAΦNE is a e^+-e^- collider, working at the energy $\sqrt{s} = m_\phi = 1.0195\,GeV$ and it is located at the INFN-LNF of Frascati. The DAΦNE Accelerator Complex consists of a linear accelerator, a damping ring, nearly 180 m of transfer lines, two storage rings that intersect at two points, a beam test area (BTF) and three syncrotron light lines (see Fig.1).

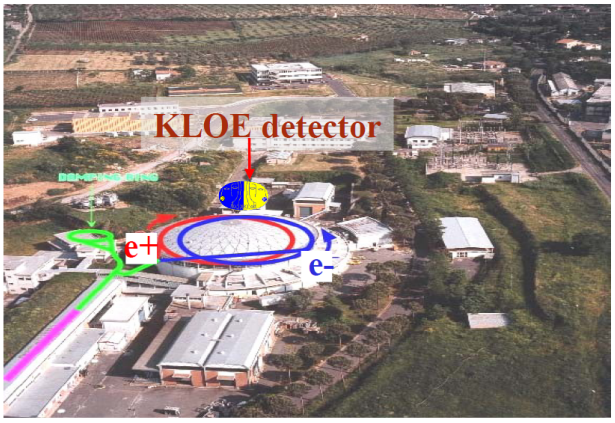

Figure 1: *DAΦNE accelerator complex*

The KLOE detector is made up of a large cylindrical drift chamber (DC, see Fig.2 left side), surrounded by a lead scintillating fiber electromagnetic calorimeter (EMC, see Fig.2 right side). A superconducting coil around the EMC provides a 0.52 T magnetic field. The EMC provides measurement of photon energies, impact point and an accurate measurement of the arrival time of particles. The DC is well suited for tracking of the particles and charged vertices reconstruction. The calorimeter is divided into a barrel and two end–caps and covers 98% of the full solid angle. The modules

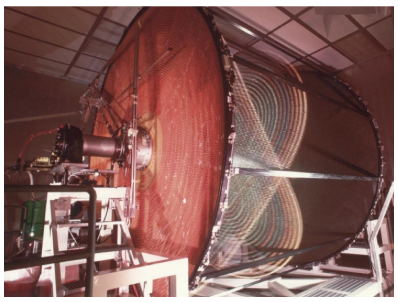
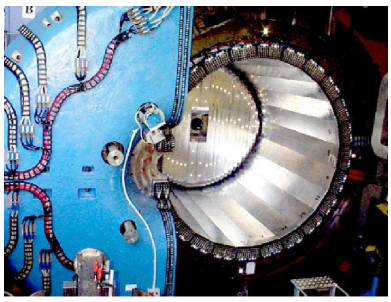

Figure 2: *Left side: KLOE drift chamber Right side: KLOE calorimeter*

are read out at both ends by 4880 photo–multipliers. Energy and time resolutions are $\sigma_E/E = \ 5.7\%/\sqrt{E(GeV)}$ and $\sigma_t = 57\,ps\ /\sqrt{E(GeV)}\ \oplus 50\,ps$, respectively. The all-stereo drift chamber, $4\,m$ in diameter and $3.3\,m$ long, is provided of 12000 sense wires, is made of carbon fiber-epoxy composite and operates with a light gas mixture (90% helium, 10% isobutane). The position resolutions are about $\sigma_{xy} = 150\,\mu m$ and $\sigma_z = 2\,mm$. The momentum resolution is $\sigma_{p_\perp}/p_\perp > 0.4\%$ for large angle tracks. Vertices are reconstructed with a spatial resolution of about $3\,mm$.

3 Event Selection

The analysis described in the following is based on the KLOE pion form factor measurement [15]. The data sample consists of $239.29\,pb^{-1}$ of data taken in year 2002. The event selection requires:

- two charged tracks with $50^\circ < \theta_\mu < 130^\circ$ (wide cones in Fig.3 a))
- one photon within a cone of $\theta_\gamma < 15^\circ$ ($\theta_\gamma > 165^\circ$) around the beamline (narrow cones in Fig.3 a))

The photon is not detected, its direction is reconstructed from event kinematics: $\vec{p}_\gamma \simeq \vec{p}_{miss} \equiv -\vec{p}_{\mu\mu} = -(\vec{p}_{\mu^+} + \vec{p}_{\mu^-})$. This separation of tracks and photon selection regions in the analysis greatly reduces the contamination from the resonant process $e^+e^- \to \phi \to \pi^+\pi^-\pi^0$, where the π^0 mimics the missing momentum of the photon(s), and from the final state radiation processes: $e^+e^- \to \pi^+\pi^-\gamma_{\mathrm{FSR}}$ and $e^+e^- \to \mu^+\mu^-\gamma_{\mathrm{FSR}}$. Since ISR-photons are mostly

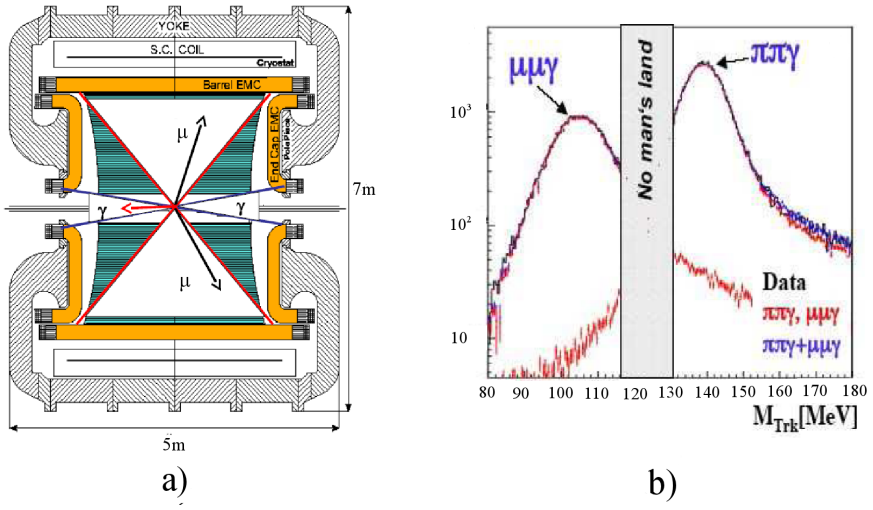

Figure 3: *a) Schematic cross-view of KLOE Detector with the selection regions for the missing momentum angle (narrow cones) and for muons track (wide cones) b) Pions and muons separation by cut on M_{Trk} variable*

collinear with the beam line, a high statistics for the ISR signal events remains. Backgrounds contributions coming from:

1. $e^+e^- \to \pi^+\pi^-\gamma(\gamma)$
2. $e^+e^- \to \Phi \to \pi^+\pi^-\pi^0$
3. $e^+e^- \to e^+e^-\gamma(\gamma)$

were separated applying kinematical cuts in the $M_{\mathrm{T}rk} - M^2_{\pi\pi}$ plane (for the definition of M_{trk} variable see later). A particle identification estimator (PID), based on a pseudo-likelihood function using the time-of-flight and calorimeter information, was used to suppress radiative Bhabha events [15, 16, 17]. Finally pions and muons are separated by a cut on the trackmass variable $M_{\mathrm{T}rk}$:

- muons are selected with $80 < M_{\mathrm{T}rk} < 115$ MeV,
- pions are selected with $M_{\mathrm{T}rk} > 130$ MeV.

The M_{Trk} variable is computed from energy and momentum conservation, assuming the presence of an unobserved photon and that the tracks belong to

particles of the same mass:

$$\left(\sqrt{s} - \sqrt{|\mathbf{p}^+|^2 + M^2_{\rm Trk}} - \sqrt{|\mathbf{p}^-|^2 + M^2_{\rm Trk}}\right)^2 - \left(\mathbf{p}^+ + \mathbf{p}^-\right)^2 = 0 \qquad (2)$$

where $\mathbf{p}^{\pm}$ is the measured momentum of the positive (negative) particle, and only one of the four solutions has physical meaning. In Fig. 3 b) is reported the separation between the $\mu^+\mu^-\gamma$ and $\pi^+\pi^-\gamma$ distributions by M_{Trk} cut. The gap between the two selections has been chosen to reduce the mutual contamination of the two samples.

4 Background Contributions

The contributions of background channels surviving the $\mu^+\mu^-\gamma$ selection, (see section 3), are obtained by fitting in slices of $M^2_{\mu\mu}$ the M_{Trk} distribution for data as a superposition of signal and background distributions.

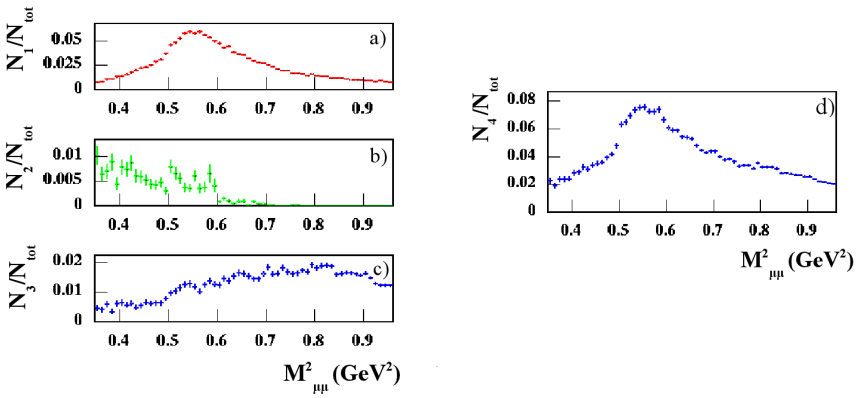

Figure 4: *a) $\pi^+\pi^-\gamma$ background contribution b) $\pi^+\pi^-\pi^0$ background contribution c) $e^+e^-\gamma$ background contribution d) sum of the three relative background contributions a), b) and c). N_1, N_2, N_3 are the background event numbers related to the above mentioned 1., 2., 3. channels, respectively; N_4 represents their sum; N_{tot} is the total number of events found in each bin of $M^2_{\mu\mu}$*

For each background channel, the fit results in normalization parameters,

called weights, $w_{ch}(j)$, produced for each slice of $M^2_{\mu\mu}$. The $M_{\mathrm{T}rk}$ distribution for $\mu^+\mu^-\gamma$, $\pi^+\pi^-\gamma$, $\pi^+\pi^-\pi^0$ were extracted by Monte Carlo calculation (MC). Since the $e^+e^-\gamma$ background is much larger, at percent level, its contribution was estimated directly from data. In Fig. 4 the contributions of the three background channels normalized to the total number of events, as well as their sum, are shown. Since in the ρ region the $\pi^+\pi^-\gamma$ cross section is about one order of magnitude greater than the $\mu^+\mu^-\gamma$ one, it is crucial to to keep under control the $\pi^+\pi^-\gamma$ $M_{\mathrm{T}rk}$ tail in the region below $125\,MeV$. For this reason, a tuning of the $M_{\mathrm{T}rk}$ tail using a control sample of $70\,pb^{-1}$ of $\Phi \to \pi^+\pi^-\pi^0$ was also applied.

4.1 Cut on the σ_{MTRK}

A further separation between pions and muons was performed by a cut on the σ_{MTRK} variable which parametrize the quality of the fit of the tracks, as explained in the reference [15]. In Fig. 5a) are reported the $\pi^+\pi^-\gamma$ (black) and

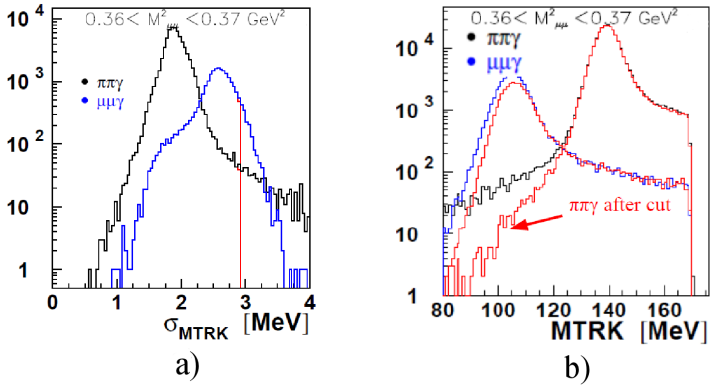

Figure 5: *a) σ_{MTRK} distribution for one $M^2_{\mu\mu}$ slice of $\pi^+\pi^-\gamma$ (black) and $\mu^+\mu^-\gamma$ (blue); in red a possible cut value is shown b) effect of σ_{MTRK} cut on M_{Trk} distributions for one slice of $M^2_{\mu\mu}$; black and blue histograms represent the $\pi^+\pi^-\gamma$ and $\mu^+\mu^-\gamma$ M_{Trk} distributions without σ_{MTRK} cut; red histograms are obtained after applying σ_{MTRK} cut*

$\mu^+\mu^-\gamma$ (blue) σ_{MTRK} distributions for one slice of $M^2_{\mu\mu}$. Figure 5b) shows the effects of σ_{MTRK} cut (red) on $M_{\mathrm{T}rk}$ distribution for one slice of $M^2_{\mu\mu}$. As it is possible to see, there is a significant reduction (up to a factor 2) of the $\pi^+\pi^-\gamma$

contamination in the $\mu^+\mu^-\gamma$ M_{Trk} region, with a consequent improvement in π/μ separation. The cut was optimized in order to keep the signal ($\mu^+\mu^-\gamma$) at a level of about 70% .

4.2 Absolute Cross Section of $\mu^+\mu^-\gamma$

Once the Data/MC corrections have been applied, the $\mu^+\mu^-\gamma$ cross section was extracted by subtracting the residual background to the observed spectra and dividing it for efficiencies and luminosity.

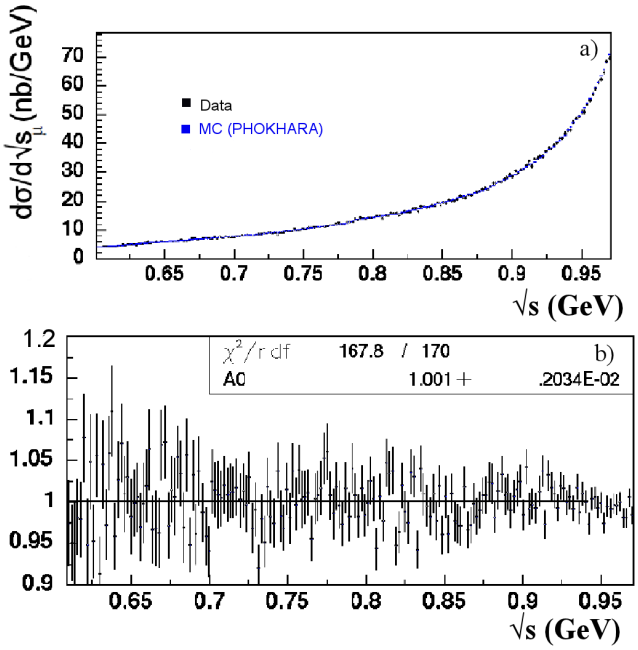

Figure 6: *a) Comparison of data (black points) and MC (blue points) of $\mu^+\mu^-\gamma$ absolute cross section b) ratio of data and MC PHOKHARA prediction*

The absolute cross section is in good agreement with the PHOKHARA prediction [18] as reported in Fig. 6.

5 Upper Limit Extraction on ε^2

To extract the upper limit (U.L.) on ε^2 the TLimit Root Class [19], based on the confidence level signal (CLS) technique [20] was used. The observed spectrum, that is the raw spectrum after offline background filter efficiency (`FILFO`) corrections (which are at percent level) and background subtraction, was used as "data" input of TLimit procedure. As "background" input was used the MC PHOKHARA spectrum properly normalized to the raw spectrum. A systematic error of $\sim 2\%$ on background was also applied.

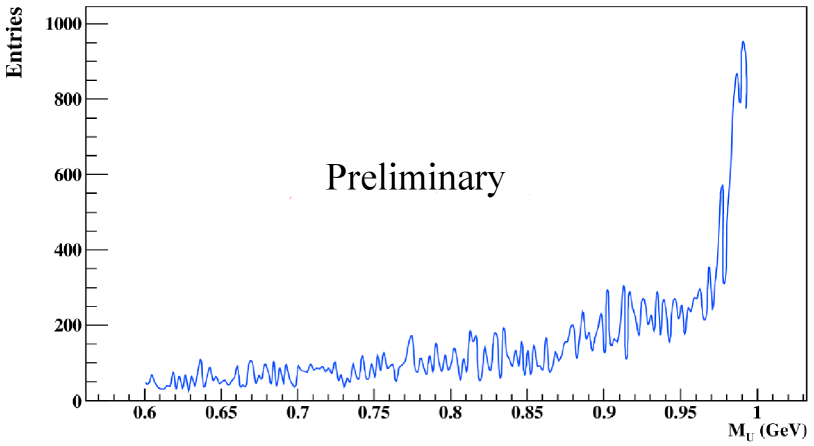

Figure 7: *Exclusion plot on number of signal events at* 90% *of C.L.*

In Fig. 7 the exclusion plot on number of signal events at 90% of confidence level (C.L.) in the energy range between 600 and 1000 MeV is shown.

The U.L. on the kinetic mixing parameter ε^2 was extracted using the following formula [21]:

$$\varepsilon^2 = \frac{\alpha^{'}}{\alpha} = \frac{N_{CLS}/(\epsilon_{eff} \cdot L)}{H \cdot I} \tag{3}$$

where N_{CLS} is the number of entries of signal hypothesis excluded as fluctuations at the 90% C.L.; ϵ_{eff} represents the efficiency and acceptance corrections; L is the integrated luminosity ($L = 239,29\, pb^{-1}$); H is the radiator function given by:

$$H = \frac{d\sigma_{\mu^+\mu^-\gamma}/d\sqrt{s_\mu}}{\sigma(e^+e^- \to \mu^+\mu^-, s_\mu)} \tag{4}$$

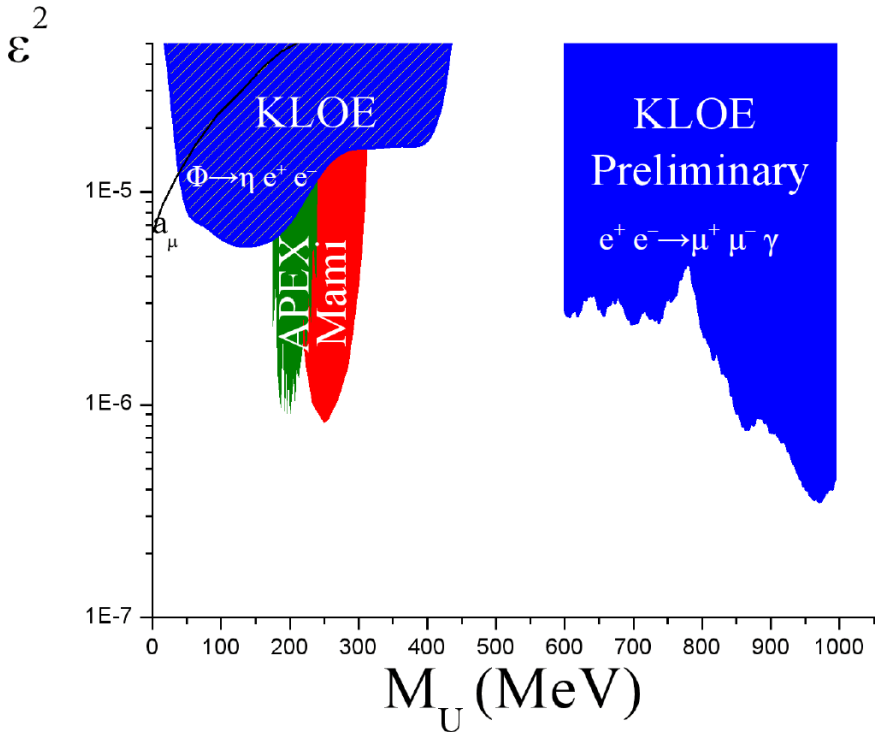

Figure 8: *Exclusion Plot on ε^2 in comparison with the existing limits in the $0 - 1000\,MeV$ range*

where $d\sigma_{\mu^+\mu^-\gamma}/d\sqrt{s_\mu}$ is the partial cross section of $e^+e^- \to \mu^+\mu^-\gamma(\gamma)$, s_μ is the invariant mass of muons, $\sigma(e^+e^- \to \mu^+\mu^-, s_\mu)$ is the total cross section of $e^+e^- \to \mu^+\mu^-$ process; the quantity I is given by the following integral:

$$I = \int_i \sigma_U^{\mu\mu}\, ds_i \tag{5}$$

where $\sigma_U^{\mu\mu} = \sigma(e^+e^- \to U \to \mu^+\mu^-, s)$ is the total cross section of U boson production decaying in the $\mu^+\mu^-$ channel, $s = M_U^2$, and i is the mass bin number. In Fig.8 the kinetic mixing parameter ε^2 obtained by formula 3, in the $600-1000\,MeV$ range and the other existing limits are presented. The blue area is the present measurement derived using the $e^+e^- \to \mu^+\mu^-\gamma$ channel, the U.L. is between $2.6 \cdot 10^{-6}$ and $3.5 \cdot 10^{-7}$, it is clearly visible the reduction

of the sensitivity due to ρ meson at about $0.77\,GeV$. The red area represents the Mami results [22], the dark green area refers to the Apex measure [23] and finally, the blue shaded area shows the KLOE U.L. in the $0 - 460\,MeV$ region calculated using the Dalitz Φ decay [24]. The black line represents the ε^2 values consistent with a U boson contribution to the muon magnetic moment anomaly a_μ.

6 Conclusions

$239.29\,pb^{-1}$ of 2002 KLOE data were used to search for light vector boson in the $e^+e^- \to \mu^+\mu^-\gamma$ channel. No U boson evidence was found and an U.L. has been extracted on coupling factor ε^2 in the energy range between 600 and $1000\,MeV$. The preliminary results exclude a possible effect of U boson existence on the a_μ in the investigated energy range between 600 and 1000 MeV. An extension of the muon acceptance selection and full statistics analysis ($2.5\,fb^{-1}$) is planned to have the possibility to explore the muon spectrum at lower invariant mass region, extending the present measurement and increasing the sensitivity of about a factor 3.

References

1. O. Adriani *et al.*, Nature **458**, 607 (2009).
2. P. Jean *et al.*, Astronomy Astrophysics **407**, L55 (2003).
3. J. Chang *et al.*, Nature **456**, 362 (2008).
4. F. Aharonian *et al.*, Phys. Rev. Lett. **101**, 261104 (2008).
5. A. A. Abdo *et al.*, Phys. Rev. Lett. **102**, 181101 (2009).
6. R. Barnabei *et al.*, Eur. Phys. J. C **56**, 333 (2008).
7. C. Boehm, P. Fayet, Nucl. Phys. B **683**, 259 (2004).
8. M. Pospelov, A. Ritz, M.B. Voloshin, Phys. Lett. B **662**, 53 (2008).
9. M. Pospelov, A. Ritz, Phys. Lett. B **671**, 391 (2009).
10. N. Arkani-Hamed, D.P. Finkbeiner, T.R. Slatyer *et al.*, Phys. Rev.D **79**, 015014 (2009).

11. I. Cholis, G. Dobler, D.P. Finkbeiner *et al.*, Phys. Rev. D **80**, 123518 (2009).

12. Y. Mambrini, J. Cosmol. Astropart. Phys. **022**, 1009 (2010).

13. L. Barzè *et al.*, Eur. Phys. J. C **71**, 1680 (2011).

14. B. Holdom, Phys. Lett. B **166**, 196 (1986).

15. D. Babusci *et al.*, arXiv:1212.4524 [KLOE/KLOE2 Collaboration].

16. F. Ambrosino *et al.*, Phys. Lett. B **670**, 285 (2009) [KLOE Collaboration].

17. F. Ambrosino *et al.*, Phys. Lett. B **700**, 102 (2011) [KLOE Collaboration].

18. H. Czyż *et al.*, Eur. Phyis. J. C **39** 411 (2005).

19. http://root.cern.ch/root/html/TLimit.html.

20. G. C. Feldman, R. D. Cousins, Phisical Rev. D **57**, 3873 (1998).

21. G. Venanzoni, KLOE2 Internal Note K2ID-12,

    `http://www.lnf.infn.it/kloe2/index.php?lv1=documents&lv2=list&lv3=private&lv4=k2id.`

22. M. Merkel *et al.*, Phys. Rev. Lett. **106**, 251802 (2011).

23. S. Abrahamyan *et al.*, Phys. Rev. Lett. **107**, 191804 (2011).

24. D. Babusci *et al.*, arXiv:1210.3927 [KLOE/KLOE2 Collaboration].